

**Magnetic excitations in long-range stripe-ordered Pr<sub>2</sub>NiO<sub>4+δ</sub>**Avishek Maity<sup>1,\*</sup>, Rajesh Dutta<sup>2,3,†</sup>, Anna Marsicano<sup>4</sup>, Andrea Piovano<sup>5</sup>, J. Ross Stewart<sup>6</sup> and Werner Paulus<sup>4,‡</sup><sup>1</sup>Heinz Maier-Leibnitz Zentrum (MLZ), Technische Universität München, 85747 Garching, Germany<sup>2</sup>Institut für Kristallographie, RWTH Aachen Universität, 52066 Aachen, Germany<sup>3</sup>Jülich Centre for Neutron Science (JCNS) at Heinz Maier-Leibnitz Zentrum (MLZ), 85747 Garching, Germany<sup>4</sup>Institut Charles Gerhardt Montpellier, Université de Montpellier, CNRS-ENSCM, 34095 Montpellier, France<sup>5</sup>Institut Laue-Langevin, 71 Avenue des Martyrs, 38000 Grenoble, France<sup>6</sup>ISIS Neutron and Muon Source, Rutherford Appleton Laboratory, Didcot OX11 0QX, United Kingdom

(Received 19 October 2020; revised 25 January 2021; accepted 22 February 2021; published 2 March 2021)

We report an inelastic neutron scattering study on the magnetic excitations of Pr<sub>2</sub>NiO<sub>4+δ</sub> ( $\delta \sim 0.24 \pm 0.01$ ) at  $T = 10$  K. Spin stripe ordering becomes pronounced below  $\sim 220$  K with an incommensurability  $\epsilon \approx 0.346$ , and a strong influence of interstitial oxygen is identified on establishing a long-range spin stripe ordering. Apart from the Goldstone modes emerging from the magnetic satellites ( $\mathbf{q}_m$ ), multiple homologous modes are observed along the spin stripe modulation separated by  $\Delta\mathbf{q}_m \approx 0.076$  in reciprocal lattice units, which is interpreted by the internal periodicity of the long-range ordered discommensurated spin stripes.

DOI: [10.1103/PhysRevB.103.L100401](https://doi.org/10.1103/PhysRevB.103.L100401)

Dynamics of spin stripes in the hole-doped lanthanide ( $Ln$ ) based 214-type nickelates ( $Ln_{2-x}Sr_xNiO_{4+\delta}$ ) [1–8] remains very interesting and nontrivial phenomena, especially considering the presence of similar electronic ordering in the normal state of high- $T_c$  superconducting 214 cuprates [9]. Hole doping by Sr or O is electronically equivalent, though it is important to note that Sr doping is done at the expense of incorporating disorder as immobile Sr randomly occupies the  $Ln$  sites without getting ordered in the lattice. In comparison, excess O occupies the interstitial sites and remains mobile in the lattice even below room temperature (RT) causing a long-range O ordering along with the localization of induced holes [10]. Neutron scattering studies in  $La_2NiO_{4+\delta}$  reveal the interstitial oxygen orders in three dimensions [11]. Such oxygen ordering has been also observed in the oxygen doped high- $T_c$   $La_2CuO_{4+\delta}$ , and plays an important role in the enhancement of the superconducting transition temperature  $T_c$  and in magnetic correlations [12,13]. In  $La_2NiO_{4+\delta}$ , the interstitial oxygen induced holes order simultaneously with the spins in a cooperative manner [14,15]. Holes tend to organize in the form of stripes through the Ni sites rather than the O sites below spin ordering temperature [10]. In the last three decades a significant number of investigations have been directed towards the magnetic excitations of mostly Sr-doped samples [2–7] in comparison to the O-doped samples [1,8]. In O-doped samples stripes are expected to be long-range, hence can give very interesting and complementary results compared to Sr-doped samples in which the unavoidable disorder introduced by the Sr results into a short-range stripe correlation.

Pr-based 214 nickelates are excellent candidates for accommodating higher amount of interstitial oxygen ( $O_{int}$ ) with  $\delta_{max} \approx 0.25$  in comparison to the La-based nickelates [16].  $O_{int}$  in Pr<sub>2</sub>NiO<sub>4+δ</sub> are highly mobile inside the lattice and orders three dimensionally in long-range already at RT [17]. This makes Pr<sub>2</sub>NiO<sub>4+δ</sub> a promising candidate for investigating the effect of  $O_{int}$ , and in particular the effect of expected long-range stripe ordering on the magnetic excitations of hole-doped 214 nickelates.

In this letter, we present an inelastic neutron scattering (INS) study of the magnetic excitations in a O-doped Pr<sub>2</sub>NiO<sub>4+δ</sub> single crystal measured up to energy transfer of  $\sim 90$  meV at  $T = 10$  K. We have discussed our intriguing observation of multiple modes in the magnetic excitations using linear spin wave theory (LSWT) based calculations. Our results give an indication that long-range spin stripe ordering is seemingly imposed by the  $O_{int}$  ordering in the similar correlation length scale, and we find the internal periodicity within the discommensurated spin stripe (DCSS) unit to be responsible for the multiple homologous modes stemming from equidistant wave vectors with slowly decreasing intensity from the magnetic zone centers.

INS measurements were performed on the thermal triple-axis spectrometer (TAS) PUMA [18] at Heinz Maier-Leibnitz Zentrum, Germany, TAS IN8 [19] at the Institut Laue-Langevin, France, and on the thermal neutron time-of-flight (TOF) multichopper spectrometer MAPS [20] at the ISIS Neutron and Muon Source of the Rutherford Appleton Laboratory, UK. All the experiments have been carried out on the same single crystal of Pr<sub>2</sub>NiO<sub>4+δ</sub> with dimension  $20 \times 5 \times 5$  mm<sup>3</sup> grown by the traveling solvent floating zone method [21]. We interpret our results in a pseudotetragonal  $F4/mmm$  unit cell with lattice parameters  $a = b \approx 5.424$  Å and  $c \approx 12.44$  Å, in which the spin ordering reflections with incommensurate modulation  $\epsilon$  appear by following the stripe

\*avishek.maity@frm2.tum.de

†rajesh.dutta@frm2.tum.de

‡werner.paulus@umontpellier.fr

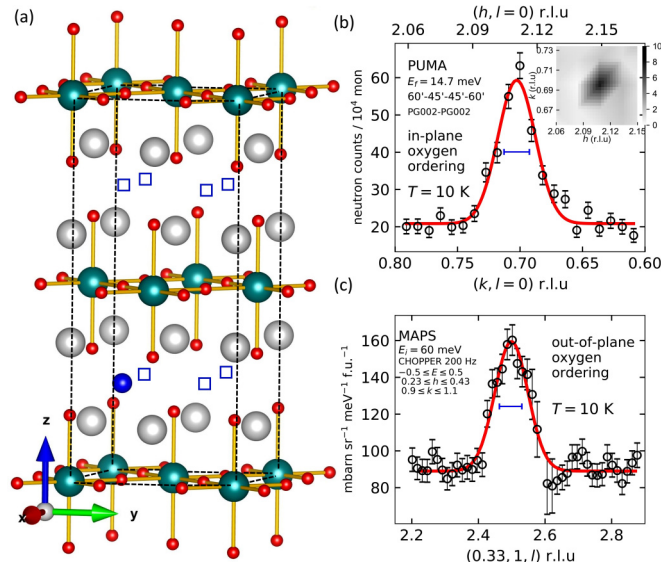


FIG. 1. (a) Structure of  $\text{Pr}_2\text{NiO}_{4+\delta}$  (Ni in dark cyan, Pr in grey, octahedrally coordinated oxygen to the Ni sites in red, and interstitial oxygen in deep blue). The chemical unit cell is indicated in black dashed lines. Squares in blue indicate the unoccupied interstitial sites ( $8f$  Wyckoff) in the unit cell. (b) Scan at 10 K along the oxygen ordering modulation through the fourth-order satellite originating from (040), (inset) RT mapping of the  $(hk0)$  plane around the same oxygen ordering satellite. (c) Line cut along  $l$  through the oxygen ordering modulation at  $l = 5/2$  in the  $(h1l)$  plane. Horizontal bars in blue represent the instrumental  $Q$  resolution for the presented scans.

ordering wave vector  $\mathbf{q}_m = (1 \pm \epsilon, 0, 0)$  [22]. All the coordinates are presented in reciprocal lattice units (r.l.u), i.e., in the units of  $(2\pi/a, 2\pi/b, 2\pi/c)$ .

The dopant oxygen ions in  $\text{Pr}_2\text{NiO}_{4+\delta}$  can occupy one of the possible eight equivalent interstitial sites  $(1/4, 1/4, 1/4)$  in a unit cell in between the  $\text{NiO}_2$  layers as presented in Fig. 1(a), and orders three dimensionally already at RT. The satellite reflections from the  $\text{O}_{\text{int}}$  ordering in the present sample have been characterized by following the convention used in the synchrotron diffraction study in Ref. [17]. The RT modulation of the oxygen ordering has been determined by mapping the  $(hk0)$  plane around the expected position of the fourth-order satellite reflection as shown in Fig. 1(b)(inset). The observed reflection position corresponds to an in-plane oxygen ordering vector  $\mathbf{q}_{\text{O}_{\text{ip}}} = (0.819 \pm 0.005, 0.521 \pm 0.005, 0)$ . No changes in the oxygen ordering modulation have been observed while cooling the sample to 10 K (with a rate 2 K/min), and this has been confirmed from a line scan through the same satellite reflection in the direction of the modulation as presented in Fig. 1(b). From the scan along  $l$  in Fig. 1(c), we confirm the presence of reflections from oxygen ordering satellites in the  $l = \text{half-integer}$  positions with the out-of-plane modulation vector  $\mathbf{q}_{\text{O}_{\text{oop}}} = (-0.25, 0.25, 0.5l)$  where  $l = \text{odd}$ . For a detailed description of the interstitial oxygen ordering, see Fig. S1 in the Supplemental Material [23]. From the scan at  $T = 10$  K in Fig. 1(b), we have obtained the in-plane oxygen order correlation length  $\xi_{\text{ip}} \approx 50 \text{ \AA}$  from the projection of the full width at half maximum (FWHM) along the  $\mathbf{q}_{\text{O}_{\text{ip}}}$ . Similarly,

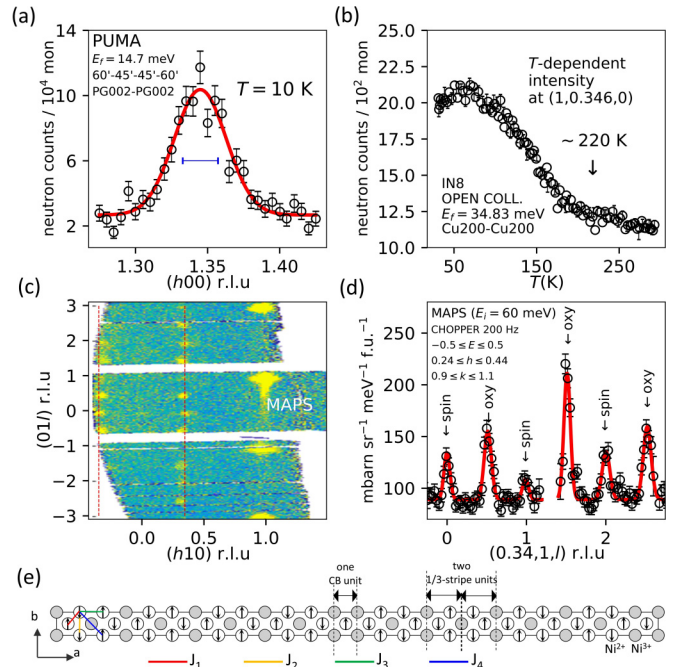


FIG. 2. (a) Elastic scan through spin peak at  $(1.346, 0, 0)$  along  $h$ . Horizontal bar in blue represents the instrumental  $Q$  resolution. (b)  $T$ -dependent magnetic intensity of the spin stripe order satellite at  $(1, 0.346, 0)$ . (c) Two-dimensional cut of  $(h1l)$  plane obtained from the MAPS data at 10 K. The  $h = \pm 0.346$  dashed lines in red corresponding to the magnetic incommensurabilities are presented to guide the eye. (d) Line cut along  $l$  through spin stripe order ( $l = \text{integer}$ ) and oxygen order ( $l = \text{half-integer}$ ) satellites. (e) DCSS unit along the  $a$  axis corresponding to  $\epsilon = 0.346$  presented for a single twin domain. For the other orthogonal twin domain the DCSS unit is exactly the same but rotated by  $90^\circ$  around the  $c$  axis. Exchange interactions are indicated by solid lines in different colors.

from the scan along  $l$  through the oxygen ordering reflection in the Fig. 1(c) we have obtained the out-of-plane oxygen order correlation length  $\xi_{\text{oop}} \approx 40 \text{ \AA}$ .

We find the spin stripe incommensurability  $\epsilon \approx 0.346$ , slightly different from the commensurate  $1/3$  spin stripes, as can be seen from the elastic scan around the antiferromagnetic (AFM) zone center in Fig. 2(a). The spin stripe ordering starts to be pronounced below  $\sim 220$  K as can be followed from the  $T$ -dependent intensity of the magnetic satellite at  $(1, 0.346, 0)$ , presented in Fig. 2(b). Following the spin discommensuration proposed by Tranquada *et al.* [15] and Yoshizawa *et al.* [24],  $\epsilon \approx 0.346$  can be obtained from a mixture of  $m = 8$  units of  $1/3$  stripe and  $n = 1$  unit of checkerboard (CB) using the expression  $\epsilon = (m + n)/(3m + 2n)$ . The corresponding DCSS unit is presented in Fig. 2(e). We have observed an intensity ratio of  $\sim 2.5$  for the spin satellites with  $l = \text{even}$  and  $l = \text{odd}$  as can be seen in the Fig. 2(d). This corresponds to a shift of the discommensurated  $\text{NiO}_2$  plane at  $z = 1/2$  by  $a/2$  in the three-dimensional DCSS model as have been similarly explained in Refs. [25,26]. For a detailed description on the optimization of three-dimensional DCSS model, see Fig. S2 in the Supplemental Material [23]. Please note that the reflections at the  $l = \text{half-integer}$  positions are solely contributed by  $\text{O}_{\text{int}}$  ordering at  $h \approx 0.33$  r.l.u whereas the  $l = \text{integer}$

reflections originate from the spin stripe ordering, and appear at a slightly higher value of  $h = 0.346$  r.l.u. as can be noticed from the map in Fig. 2(c). From the scan in Fig. 2(a), we have obtained the in-plane spin stripe correlation length  $\xi_{ip} \approx 47 \text{ \AA}$ , almost similar to the in-plane oxygen correlation length  $\xi_{ip}$ . Likewise, we find the out-of-plane spin correlation length  $\xi_{oop}$  is also similar to the corresponding  $O_{\text{int}}$  correlation length  $\xi_{oop}$ , as can be realized from the FWHMs of the oxygen and spin stripe ordering peaks in Fig. 2(d).

Since the  $O_{\text{int}}$  already orders at RT, the three-dimensional matrix of the  $O_{\text{int}}$  may have a strong influence on localizing the holes as reflected by almost similar correlation lengths of the spin stripe ordering and oxygen ordering at low temperature. In this regard, it is important to draw a comparison with the Sr-doped samples. In the nominal half-doped sample  $\text{Pr}_{1.5}\text{Sr}_{0.5}\text{NiO}_4$  [26], the observed in-plane and out-of-plane spin stripe correlation lengths ( $\sim 19 \text{ \AA}$  and  $\sim 8.4 \text{ \AA}$ , respectively) are relatively short in comparison to the almost electronically equivalent oxygen doped samples  $\text{Pr}_2\text{NiO}_{4+\delta}$  with  $\delta \sim 0.25$ . Consequently we find the O-doped sample in this work is perfectly suitable for investigating the effect of long-range spin stripe ordering in the spin wave dispersion.

Figure 3 presents a series of constant- $E$  scans through the magnetic zone centers at  $(3, \pm\epsilon, 0)$  from PUMA and IN8 data along  $k$  and also constant- $E$  profiles along  $h$  at  $(1 \pm \epsilon, 0, 0)$  from MAPS data (see Fig. S3 in the Supplemental Material [23]). To determine the eigenvectors of the spin wave dispersion, all the scans have been fitted with multiple Gaussian profiles. Since the scans cover a large  $Q$  range, the background is nontrivial, and hence the background has been kept constant in all the fits without performing any correction. As can be clearly evidenced from the constant- $E$  scan at 17 meV (with tight collimation instrument  $Q$  resolution  $\sim 0.02 \text{ \AA}^{-1}$ ), multiple (eight in here) peaks are present, although typically only two peaks are expected at  $(3, 0.308, 0)$  and  $(3, 0.384, 0)$  from the two branches of the conventional Goldstone mode dispersing from the magnetic satellite at  $\mathbf{q}_m = (3, 0.346, 0)$ . This observation also holds for other scans presented in Fig. 3, and in general the observed intensities of the side peaks seem to decrease on both sides of the expected branches of the Goldstone modes dispersing from the  $(3, \pm 0.346, 0)$  and  $(1 \pm 0.346, 0, 0)$ , giving a notion of multiple modes in the spin wave dispersion.

To explain the observed spin excitation spectra, we have performed LSWT based calculation via SPINW code [27] using the generalized Heisenberg spin-only Hamiltonian given as

$$H = \sum_{i,j} J_{ij}(\vec{S}_i \cdot \vec{S}_j), \quad (1)$$

where the indices  $i$  and  $j$  run over all the lattice sites of  $\text{Ni}^{2+}$ ,  $J_{ij}$  represents all possible isotropic Heisenberg exchange interactions among  $\text{Ni}^{2+}$  spins  $\vec{S}_i$  and  $\vec{S}_j$  as denoted by the solid lines in different colors  $J_1$  to  $J_4$  in Fig. 2(e). We have incorporated the site centered DCSS unit corresponding to the  $\epsilon = 0.346$  for our spin wave calculation taking into account the orthogonal twin domain. For details on the effect of twin volume fraction on spin wave dispersion, see Fig. S4 in the

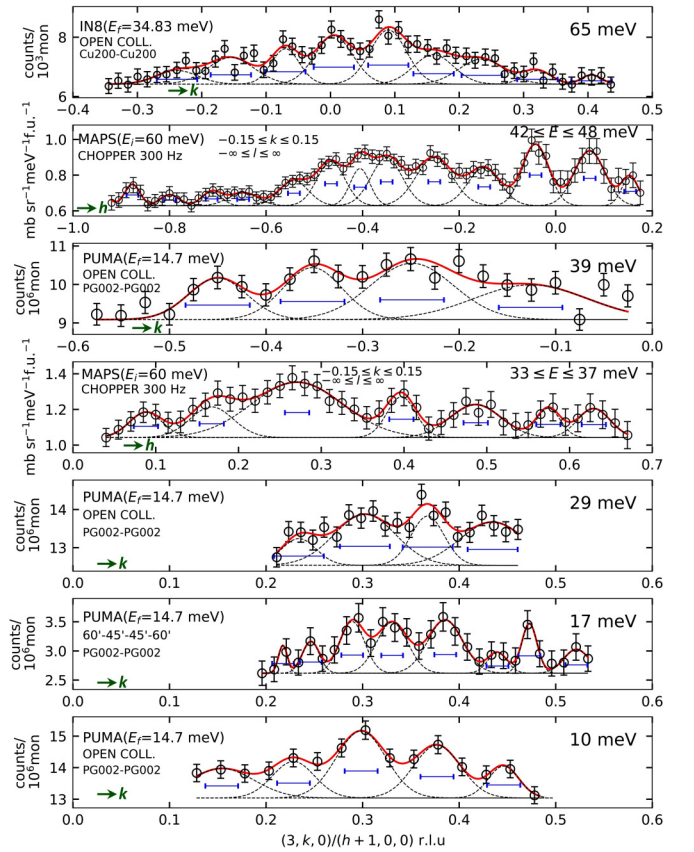


FIG. 3. Constant- $E$  scans performed at 10 K up to 65 meV on both sides of the AFM zone centers along  $h$  and  $k$  as indicated in the scans. Solid lines in red represent the cumulative fit and dashed lines in black show Gaussian fit components. Horizontal bars in blue represent the instrumental  $Q$  resolution. The text in the left inset shows instrument configurations (e.g., fixed final ( $E_f$ ) or initial ( $E_i$ ) energy of neutrons, collimation, monochromator-analyzer, chopper frequency for TAS and TOF) with which the scans have been performed.

Supplemental Material [23]. In addition to the in-plane interactions, we have considered an out-of-plane interaction  $J_{\perp}$  in between the  $\text{Ni}^{2+}$  spins within the nearest layers of discommensurated  $\text{NiO}_2$  planes. From a least-squares fit of the measured wave vectors we have obtained the refined in-plane exchange interactions  $J_1 \approx 23.13 \pm 1.56$ ,  $J_2 \approx -0.41 \pm 0.2$ ,  $J_3 \approx 14.38 \pm 1.12$ , and  $J_4 \approx 7.0 \pm 1.8$  meV. We have achieved the best match of the measured dispersion with the out-of-plane interaction  $J_{\perp} \approx 0.4 \pm 0.06$  meV. However, we want to make a remark that due to the inherent complexity of the underlying spin microstructure in the DCSS unit, and also due to the presence of a large number of peaks in the inelastic scans, the errors in estimating the exchange interactions might be significant in comparison to the above-mentioned values obtained from the dispersion fit.

The calculated spin wave spectra presented in Fig. 4(a) interestingly shows parallel branches from multiple modes in the spin wave dispersion stemming equidistantly from the side of the magnetic zone centers along the stripe modulation and separated by  $\Delta\mathbf{q}_m = 0.076$  r.l.u., which can also be seen from the scan at 10 meV presented in Fig. 3. The measured inelastic peaks along  $h$  and  $k$  from the scans in Fig. 3 [also from some

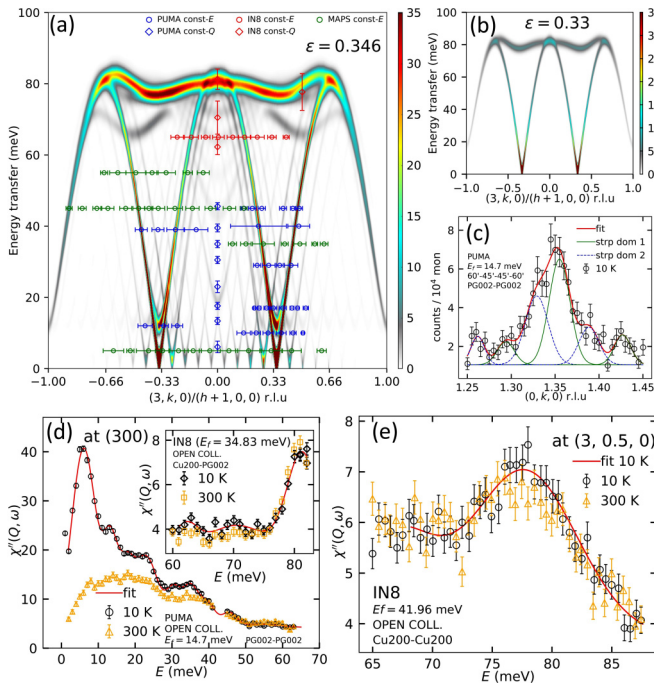


FIG. 4. (a) Spin wave dispersion calculated from SPINW. The measured peak positions from the inelastic scans have been overlaid on the calculated dispersion. Horizontal and vertical bars represent the FWHMs of the peaks in  $Q$  and  $E$ , respectively. (b) Calculated spin wave dispersion for  $1/3$  stripe. (c) Elastic scan through the magnetic satellite reflection at  $(0, 1.346, 0)$ . (d), (e) Bose corrected constant- $Q$  scans at  $(3, 0, 0)$  and at  $(3, 0.5, 0)$ . No background correction has been performed for the presented scans. All fits have been done keeping the background constant.

additional constant- $E$  scans (not shown)] are overlaid on the calculated spin wave dispersion, which shows an ample agreement between the experiments and calculation. From the measurements along the  $h$  and  $k$  directions, we have observed similar spin wave velocities ( $\approx 347$  meV $\text{\AA}$ ) without presenting any noticeable anisotropy of the spin wave dispersion in the  $(hk0)$  plane. It is noteworthy that for the closest commensurate case of  $1/3$  stripe where the spin stripe unit is much smaller in dimension and contains only a single  $1/3$  stripe unit, such a spin wave dispersion with multiple homologous modes is not observed as expected [4]. For a direct comparison, the spin wave spectra for an ideal  $1/3$  stripe is presented in Fig. 4(b) taking the same  $J$  parameters used in this present work. This clearly suggests that discommensuration, i.e., the mixing of stripe and CB units, can highly influence the spin excitation spectra. To best of our knowledge, such a spin wave dispersion of multiple homologous modes has not been reported so far in the magnetic excitations of 214-type nickelates. Our spin discommensuration model for the observed incommensurability reveals that the minimal internal periodicity within the DCSS unit might be responsible for the multiple modes, and given the long-range spin stripe correlations the modes have been experimentally observed as SPINW also considers long-range spin ordering for the LSWT calculations. We have observed the separation between the modes depends on the number of  $1/3$  stripe ( $m$ ) and CB ( $n$ ) units present in the DCSS unit,

and can be expressed empirically as  $\Delta\mathbf{q}_m = 2/(3m + 2n)$  in the range  $1/3 < \epsilon < 1/2$ . This is also valid for the calculated spin excitation spectra presented in Refs. [25,26] for the spin stripe discommensurated Sr-doped samples with  $\epsilon = 0.4$  and  $0.461$ , where the observed  $\Delta\mathbf{q}_m$  were  $0.4$  and  $0.154$  r.l.u., respectively. But the multiple modes were not observed experimentally in those Sr-doped samples due to the relatively short-range nature of the spin stripe correlations, clearly demonstrating the effect of long-range spin stripe ordering in the spin excitations of  $\text{Pr}_2\text{NiO}_{4+\delta}$ .

Nonetheless, the multiple modes, as have been interpreted to originate from the internal periodicity, should also indicate the presence of multiple magnetic peaks in the elastic line separated by  $\Delta\mathbf{q}_m = 0.076$  r.l.u., which has been confirmed by a scan through the magnetic zone center at  $(0, 1.346, 0)$  as presented in Fig. 4(c). The dashed lines in blue and solid lines in green indicate the peaks from the two unidirectional spin stripe domains [28] present in this compound. At this zone center the separation between the corresponding peaks from the unidirectional stripe domains is  $\approx 0.02$  r.l.u. along  $k$  which depends on the twinning and related orthorhombicity of the compound. The first side peaks corresponding to each stripe domain are clearly visible on both sides of the main magnetic peaks in the  $Q$  range of the scan. In addition, we have performed some constant- $Q$  scans at  $(300)$  and  $(3, 0.5, 0)$  as presented in Figs. 4(d) and 4(e) to determine the optical like modes at the AFM zone center and also to catch the top of the spin wave dispersion. The  $T$  dependence clearly shows the magnetic origin of the optical like modes. The strong peak at  $\sim 6$  meV in the constant- $Q$  scan at  $(300)$  is from the crystalline electric field excitations as reported similarly in Refs. [25,26]. The modes at  $(300)$  in the energy range  $81$  meV may have been affected by the overlap of phonon. Such a high energy phonon has been reported in the similar compound [29]. However, this does not affect our discussion on the experimentally observed multiple modes in the spin wave dispersion in  $\text{Pr}_2\text{NiO}_{4+\delta}$ .

In summary, we report a detailed study on the effect of interstitial oxygen ordering and magnetic excitations in a oxygen doped single crystal of  $\text{Pr}_2\text{NiO}_{4+\delta}$ . Interstitial oxygen ordering gets established already at room temperature and the ordering remains unchanged down to base temperature. The observed spin stripe correlation length is quite high compared to the electronically equivalent Sr-doped samples  $\text{Pr}_{1.5}\text{Sr}_{0.5}\text{NiO}_4$  [25,26]. The spin stripe ordering in  $\text{Pr}_2\text{NiO}_{4+\delta}$  shows almost similar correlation length as that of  $\text{O}_{\text{int}}$  ordering. This gives an indication that the oxygen ordering may have a strong influence on localizing the induced holes almost in the same length scale. Nonetheless, the long-range spin stripe correlation brings an interesting feature to the magnetic excitations. We have observed multiple modes stemming due to the internal periodicity of the DCSS unit, and the linear spin wave calculation which assumes also that long-range ordering gives an impressive agreement of the observed multiple modes. Our study sufficiently demonstrate the importance of interstitial oxygen ordering on establishing a long-range spin stripe ordering as validated by the LSWT calculation in the DCSS model and by the presence of multiple modes in the magnetic excitations of  $\text{Pr}_2\text{NiO}_{4+\delta}$ . The direct observation of the multiple modes in the magnetic excitations provides

further evidence that consideration of the DCSS model with a mixture of CB and stripe units is appropriate for description of these hole-doped stripe phases of 214-type nickelates. However, further INS studies on the samples with even higher spin stripe correlation length would be desirable to better constrain the model parameters in the LSWT calculation via a more explicit comparison of the experimentally observed intensities of the spin wave dispersion. These results will have direct implications in the homologous O-doped 214 cobaltates, and especially to further understand the effect of interstitial oxygen on  $T_c$  and magnetic correlations in O-doped 214 cuprates.

MAPS data are available at ISIS Neutron and Muon Source Data Journal [30] and ILL data are available at the ILL Data Portal [31].

A.M. and R.D. would like to acknowledge the financial support from Technische Universität München and RWTH Aachen Universität, respectively, for performing the measurements at MAPS and IN8. Financial support from the French National Research Agency (ANR) through the project SECTOR No. ANR-14-CE36-0006-01 is gratefully acknowledged.

- 
- [1] J. M. Tranquada, P. Wochner, and D. J. Buttrey, *Phys. Rev. Lett.* **79**, 2133 (1997).
- [2] P. Bourges, Y. Sidis, M. Braden, K. Nakajima, and J. M. Tranquada, *Phys. Rev. Lett.* **90**, 147202 (2003).
- [3] S. Anissimova, D. Parshall, G. D. Gu, K. Marty, M. D. Lumsden, S. Chi, J. A. Fernandez-Baca, D. L. Abernathy, D. Lamago, J. M. Tranquada, and D. Reznik, *Nat. Commun.* **5**, 3467 (2014).
- [4] A. T. Boothroyd, D. Prabhakaran, P. G. Freeman, S. J. S. Lister, M. Enderle, A. Hiess, and J. Kulda, *Phys. Rev. B* **67**, 100407(R) (2003).
- [5] P. G. Freeman, A. T. Boothroyd, D. Prabhakaran, C. D. Frost, M. Enderle, and A. Hiess, *Phys. Rev. B* **71**, 174412 (2005).
- [6] P. G. Freeman, S. R. Giblin, K. Hradil, R. A. Mole, P. Cermak, and D. Prabhakaran, *Phys. Rev. B* **95**, 064403 (2017).
- [7] A. T. Boothroyd, P. G. Freeman, D. Prabhakaran, A. Hiess, M. Enderle, J. Kulda, and F. Altorfer, *Phys. Rev. Lett.* **91**, 257201 (2003).
- [8] P. G. Freeman, M. Enderle, S. M. Hayden, C. D. Frost, D. X. Yao, E. W. Carlson, D. Prabhakaran, and A. T. Boothroyd, *Phys. Rev. B* **80**, 144523 (2009).
- [9] J. M. Tranquada, B. J. Sternlieb, J. D. Axe, Y. Nakamura, and S. Uchida, *Nature (London)* **375**, 561 (1995).
- [10] P. Wochner, J. M. Tranquada, D. J. Buttrey, and V. Sachan, *Phys. Rev. B* **57**, 1066 (1998).
- [11] J. M. Tranquada, Y. Kong, J. E. Lorenzo, D. J. Buttrey, D. E. Rice, and V. Sachan, *Phys. Rev. B* **50**, 6340 (1994).
- [12] B. O. Wells, Y. S. Lee, M. A. Kastner, R. J. Christianson, R. J. Birgeneau, K. Yamada, Y. Endoh, and G. Shirane, *Science* **277**, 1067 (1997).
- [13] Y. S. Lee, R. J. Birgeneau, M. A. Kastner, Y. Endoh, S. Wakimoto, K. Yamada, R. W. Erwin, S.-H. Lee, and G. Shirane, *Phys. Rev. B* **60**, 3643 (1999).
- [14] J. M. Tranquada, J. E. Lorenzo, D. J. Buttrey, and V. Sachan, *Phys. Rev. B* **52**, 3581 (1995).
- [15] J. M. Tranquada, D. J. Buttrey, V. Sachan, and J. E. Lorenzo, *Phys. Rev. Lett.* **73**, 1003 (1994).
- [16] M. Ceretti, O. Wahyudi, A. Cousson, A. Villesuzanne, M. Meven, B. Pedersen, J. M. Bassat, and W. Paulus, *J. Mater. Chem. A* **3**, 21140 (2015).
- [17] R. Dutta, A. Maity, A. Marsicano, M. Ceretti, D. Chernyshov, A. Bosak, A. Villesuzanne, G. Roth, G. Perversi, and W. Paulus, *J. Mater. Chem. A* **8**, 13987 (2020).
- [18] O. Sobolev and J. T. Park, *J. Large-scale Res. Fac.* **1**, A13 (2015).
- [19] A. Hiess, M. Jiménez-Ruiz, P. Courtois, R. Currat, J. Kulda, and F. Bermejo, *J. Phys.: Condens. Matter* **385-386**, 1077 (2006).
- [20] R. A. Ewings, J. R. Stewart, T. G. Perring, R. I. Bewley, M. D. Le, D. Raspino, D. E. Pooley, G. Å koro, S. P. Waller, D. Zacek, C. A. Smith, and R. C. Riehl-Shaw, *Rev. Sci. Instrum.* **90**, 035110 (2019).
- [21] O. Wahyudi, M. Ceretti, I. Weill, A. Cousson, F. Weill, M. Meven, M. Guerre, A. Villesuzanne, J.-M. Bassat, and W. Paulus, *CrystEngComm* **17**, 6278 (2015).
- [22] R. Zhong, B. L. Winn, G. Gu, D. Reznik, and J. M. Tranquada, *Phys. Rev. Lett.* **118**, 177601 (2017).
- [23] See Supplemental Material at <http://link.aps.org/supplemental/10.1103/PhysRevB.103.L100401> for more details regarding simulation of interstitial oxygen order and spin stripe order satellites, optimization of the three-dimensional DCSS model, representative sets of MAPS data, and effect of twin volume fraction on spin wave dispersion. The Supplemental Material includes Refs. [17,26].
- [24] H. Yoshizawa, T. Kakeshita, R. Kajimoto, T. Tanabe, T. Katsufuji, and Y. Tokura, *Phys. Rev. B* **61**, R854 (2000).
- [25] A. Maity, R. Dutta, and W. Paulus, *Phys. Rev. Lett.* **124**, 147202 (2020).
- [26] R. Dutta, A. Maity, A. Marsicano, J. R. Stewart, M. Opel, and W. Paulus, *Phys. Rev. B* **102**, 165130 (2020).
- [27] S. Toth and B. Lake, *J. Phys.: Condens. Matter* **27**, 166002 (2015).
- [28] M. Hücker, M. v. Zimmermann, R. Klingeler, S. Kiele, J. Geck, S. N. Bakehe, J. Z. Zhang, J. P. Hill, A. Revcolevschi, D. J. Buttrey, B. Büchner, and J. M. Tranquada, *Phys. Rev. B* **74**, 085112 (2006).
- [29] A. M. Merritt, A. D. Christianson, A. Banerjee, G. D. Gu, A. S. Mishchenko, and D. Reznik, *Sci. Rep.* **10**, 11426 (2020).
- [30] ISIS Neutron and Muon Source Data Journal at <https://doi.org/10.5286/ISIS.E.RB1920233-1>.
- [31] ILL Data Portal at <https://doi.ill.fr/10.5291/ILL-DATA.EASY-517>.